Superexchange and Dipole−Dipole Energy Transfer from the $[Cr(ox)_3]^{3-}$ of 3D Oxalate Networks to Encapsulated $[Cr(bpy)_3]^{3+}$

Vaughan S. Langford, Marianne E. von Arx, and Andreas Hauser*

Département de chimie physique, Université de Genève, 30 Quai Ernest-Ansermet, 1211 Genève 4, Switzerland

Received: April 2, 1999

Electronic energy transfer from $[Cr(ox)_3]^{3-}$ (ox = oxalate) in three-dimensional (3D) anionic oxalate networks to encapsulated $[Cr(bpy)_3]^{3+}$ (bpy = 2,2′-bipyridine) cations at 1.5 K was investigated by time-resolved luminescence spectroscopy. Two series of mixed crystals of nominal compositions $[NaAl_{1-x}Cr_x(ox)_3][Rh_{0.99}Cr_{0.01}(bpy)_3]ClO_4$ (x = 0, 0.01, 0.05, 0.1, 0.2, 0.4, 0.6, 0.8, and 1) and $[NaAl_{0.99}Cr_{0.01}(ox)_3][Rh_{1-y}Cr_y(bpy)_3]ClO_4$ (y = 0, 0.01, 0.02, 0.03, 0.04, and 0.05) were utilized. Energy transfer from $[Cr(ox)_3]^{3-}$ to $[Cr(bpy)_3]^{3+}$ occurs by two mechanisms. Rapid, short-range transfer ($k_{et} > 10^6\ s^{-1}$) is attributed to superexchange coupling between the Cr^{3+} ions via π overlap of the oxalate and bipyridine ligands. In addition, at low $[Cr(ox)_3]^{3-}$ concentrations (nominally $x = 0.01$) a very much slower process with a maximum $k_{et} \approx 200\ s^{-1}$ is identified in the time-resolved spectra and attributed to a dipole−dipole mechanism. Furthermore, the resonant $[Cr(ox)_3]^{3-}$ to $[Cr(ox)_3]^{3-}$ energy migration previously reported by von Arx et al. (*Phys. Rev.* (**1996**), *B54*, 15800) assists $[Cr(ox)_3]^{3-}$ to $[Cr(bpy)_3]^{3+}$ transfer as the $[Cr(ox)_3]^{3-}$ concentration increases.

Introduction

In 1994, Decurtins and co-workers first reported a nonphotochemical synthesis of cubic three-dimensional (3D) oxalate networks with transition-metal tris-oxalate complexes as building blocks and tris-bipyridine complexes as counterions.[1] Two years later a structure in which Cr^{3+} was present as both tris-oxalate (ox) and tris-2,2′-bipyridine (bpy) complexes of composition $[NaCr(ox)_3][Cr(bpy)_3]ClO_4$ was published.[2] The same report included a brief photophysical study of this and the similar, but doped, compound $[NaCr(ox)_3][Rh_{0.99}Cr_{0.01}(bpy)_3]ClO_4$. In the former, after 568-nm excitation into the $^4A_2 \rightarrow {}^4T_2$ band of $[Cr(ox)_3]^{3-}$, essentially all of the luminescence at 7 K arises from the $^2E \rightarrow {}^4A_2$ transition (R-lines) of $[Cr(bpy)_3]^{3+}$. A "back-of-the-envelope" estimate revealed that rapid energy transfer ($k_{et} > 10^7\ s^{-1}$) occurs from $[Cr(ox)_3]^{3-}$ to $[Cr(bpy)_3]^{3+}$. Furthermore, even with only 1% $[Cr(bpy)_3]^{3+}$ present, more than 85% of the luminescence was still due to $[Cr(bpy)_3]^{3+}$, implying rapid $[Cr(ox)_3]^{3-}$ to $[Cr(ox)_3]^{3-}$ energy migration. This was definitively demonstrated shortly afterward by von Arx et al.,[3] who in fact observed resonant energy transfer within the ^2E state of $[Cr(ox)_3]^{3-}$ in $[NaCr(ox)_3][Rh(bpy)_3]ClO_4$ at 1.5 K by using fluorescence line narrowing (FLN) techniques. At higher temperatures, phonon-assisted energy transfer becomes significant, and dominates by 4.2 K.

The present work investigates energy transfer from $[Cr(ox)_3]^{3-}$ of the 3D oxalate network to $[Cr(bpy)_3]^{3+}$ complexes that lie in the cavities. Two series of compounds were prepared, of general composition $[NaAl_{1-x}Cr_x(ox)_3][Rh_{1-y}Cr_y(bpy)_3]ClO_4$. One series kept the $[Cr(bpy)_3]^{3+}$ concentration constant at nominally $y = 0.01$ and varied the fraction of $[Cr(ox)_3]^{3-}$ (nominally x = 0, 0.01, 0.05, 0.1, 0.2, 0.4, 0.6, 0.8, and 1). The second series had a nominal $[Cr(ox)_3]^{3-}$ concentration of x = 0.01 and varied the $[Cr(bpy)_3]^{3+}$ concentration (nominally y = 0, 0.01, 0.02, 0.03, 0.04, 0.05). Low $[Cr(bpy)_3]^{3+}$ concentrations were used because significant $[Cr(bpy)_3]^{3+}$ to $[Cr(bpy)_3]^{3+}$ energy migration occurs at doping levels of $y \gtrsim 0.05$, which is observed as spectral diffusion in FLN experiments.[4] The data presented here were obtained entirely at 1.5 K in order to eliminate contributions due to the above-mentioned phonon-assisted energy transfer between $[Cr(ox)_3]^{3-}$ that occurs at higher temperatures.[3]

Experimental Section

The method used for preparation of neat $[NaCr(ox)_3][Cr(bpy)_3]ClO_4$ crystals[2] was applied to the preparation of $[NaAl_{1-x}Cr_x(ox)_3][Rh_{1-y}Cr_y(bpy)_3]ClO_4$ mixed crystals with some simple modifications. Appropriate nominal mole fractions in aqueous solution of $K_3[Al(ox)_3]\cdot 3H_2O$ to $K_3[Cr(ox)_3]\cdot 3H_2O$ and of $[Rh(bpy)_3][ClO_4]_3$ to $[Cr(bpy)_3][ClO_4]_3$ were used in place of $K_3[Cr(ox)_3]\cdot 3H_2O$ and $[Cr(bpy)_3][ClO_4]_3$ solutions, respectively. $[Cr(bpy)_3]^{3+}$ is light-sensitive, so the mixed crystals were grown in the dark. Polycrystalline products were obtained in all cases.

The approximate effective concentrations of $[Cr(ox)_3]^{3-}$ and $[Cr(bpy)_3]^{3+}$ in mixed crystals were determined by x-ray fluorescence. $[Cr(ox)_3]^{3-}$ and $[Cr(bpy)_3]^{3+}$ concentrations in samples with nominally no $[Cr(bpy)_3]^{3+}$ and $[Cr(ox)_3]^{3-}$, respectively, were analyzed first. These results are summarized in Table 1, sections (a) and (b), for the series $[NaAl_{1-x}Cr_x(ox)_3][Rh(bpy)_3]ClO_4$ with nominally $x = 0.01$ to $x = 1$ and $[NaAl(ox)_3][Rh_{1-y}Cr_y(bpy)_3]ClO_4$ with nominally $y = 0.01$ to $y = 0.05$. $[Cr(ox)_3]^{3-}$ is consistently slightly more concentrated than the nominal value. However, except for the lowest concentration the difference between nominal and effective $[Cr(ox)_3]^{3-}$ concentration is smaller than the estimated error in the determination of x. Therefore, hence forward nominal values are always quoted for the $[Cr(ox)_3]^{3-}$ concentration, except for the nominally $x = 0.01$ sample for which the effective value of 0.02 is used. $[Cr(bpy)_3]^{3+}$ has a somewhat different behavior with an effective concentration of only approximately half the nominal value in the concentration range used; e.g., the

* Author to whom correspondence should be addressed.

10.1021/jp9911301 CCC: $18.00
Published on Web 08/13/1999

TABLE 1: (a) Nominal and Effective Mole Fractions for $[Cr(ox)_3]^{3-}$ in $[NaAl_{1-x}Cr_x(ox)_3][Rh(bpy)_3]ClO_4$; (b) Nominal and Effective Mole Fractions for $[Cr(bpy)_3]^{3+}$ in $[NaAl(ox)_3][Rh_{1-y}Cr_y(bpy)_3]ClO_4$; (c) Nominal and Effective Mole Fractions for $[Cr(bpy)_3]^{3+}$ in $[NaAl_{0.98}Cr_{0.02}(ox)_3][Rh_{1-y}Cr_y(bpy)_3]ClO_4$ Mixed Crystals

	$[Cr(ox)_3]^{3-}$ (mole fraction)		$[Cr(bpy)_3]^{3+}$ (mole fraction)	
	nominal	effective	nominal	effective
(a)	0	<0.001[a]	**(b)** 0.01	0.006 ± 0.003
	0.01	0.02 ± 0.005	0.03	0.019 ± 0.004
	0.05	0.08 ± 0.02	0.05	0.027 ± 0.005
	0.1	0.12 ± 0.04	**(c)** 0	→ 0[b]
	0.2	0.25 ± 0.06	0.01	0.005 ± 0.003
	0.4	0.47 ± 0.08	0.02	0.01 ± 0.003
	0.6	0.64 ± 0.08	0.03	0.015 ± 0.004
	0.8	0.85 ± 0.08	0.04	0.02 ± 0.004
	1	1	0.05	0.025 ± 0.005

[a] Upper limit determined from optical luminescence measurements comparing this sample with the 1% $[Cr(ox)_3]^{3-}$/1% $[Cr(bpy)_3]^{3+}$ sample. [b] This sample shows no luminescence from $[Cr(bpy)_3]^{3+}$.

nominally $y = 0.01$ sample effectively has $y \approx 0.006 \pm 0.003$. Measurements on the samples used in this work containing both $[Cr(ox)_3]^{3-}$ and $[Cr(bpy)_3]^{3+}$ are consistent with the above data for the series with nominally $x = 0.01$ and $y = 0.01$ to $y = 0.05$. The effective $[Cr(bpy)_3]^{3+}$ concentrations derived by assuming $x_{eff} = 0.02$ are also shown in Table 1. In the following the $[Cr(bpy)_3]^{3+}$ concentrations quoted will always correspond to these effective values.

For spectroscopic experiments samples were affixed to small copper sheets by using rubber cement, and then mounted on a sample holder which was inserted into a liquid He cryostat (Oxford Instruments Optistat Bath). The temperature of the sample was maintained at 1.5 K by pumping on the liquid He with a rotary-vane pump (Leybold Sogevac SV25), and measured with a PID temperature controller (Oxford Instruments ITC601).

Broad-band luminescence data were obtained by exciting the sample at 568 nm (<2 mW) with a CW Ar^+/Kr^+ ion laser (Spectra Physics Stabilite 2108). Luminescence was dispersed by a 0.85-m double monochromator (Spex 1404) and detected with a cooled GaAs photomultiplier tube (RCA C31034). Individual photons were counted by using a photon counter (Stanford Research Systems SR400).

Time-resolved spectra were acquired in two time regimes, by using two different lasers in conjunction with a multichannel scaler (Stanford Research Systems SR430) for data acquisition. A frequency-doubled Nd:YAG laser (Quantel BrilliantB; fwhm pulse width ~7 ns and 20-Hz pulse repetition rate) was utilized at low power (<50 μJ/mm^2) to probe the luminescence behavior at short times. The SR430 was triggered from the timing signal for the laser's Q-switch. Full time-resolved luminescence spectra of $[Cr(bpy)_3]^{3+}$ and $[Cr(ox)_3]^{3-}$ were obtained by passing the 568-nm line of the Ar^+/Kr^+ ion laser through an acousto-optic modulator (Automates and Automatismes MT0808). Modulation pulses were generated by a function generator (Stanford Research Systems DS345), and had a width of ~12 μs and a repetition rate of ~17 Hz. A pulse from the DS345 0.5 ms before the laser pulse triggered the multichannel scaler.

A Macintosh PowerPC served to control instrumentation and gather data via a GPIB interface, using powerful software developed by Oetliker on the National Instruments LabView programming platform.[5]

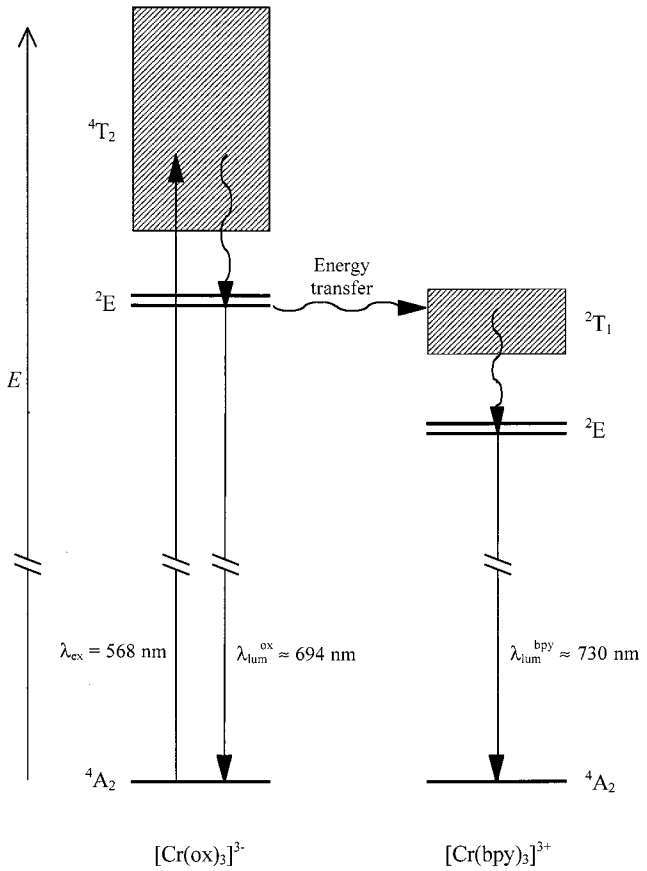

Figure 1. Low-lying electronic energy levels of $[Cr(ox)_3]^{3-}$ and $[Cr(bpy)_3]^{3+}$, showing the excitation in $[Cr(ox)_3]^{3-}$ and subsequent radiative and nonradiative processes, indicated by straight and wavy arrows, respectively.

Results

In this section we present steady-state and time-resolved luminescence data for the title compounds after a brief overview of the low-lying electronic energy levels of $[Cr(ox)_3]^{3-}$ and $[Cr(bpy)_3]^{3+}$.

Figure 1 shows the energy-level diagram for the low-lying ligand-field states of $[Cr(ox)_3]^{3-}$ and $[Cr(bpy)_3]^{3+}$ as derived from the single-crystal absorption spectra of $[NaCr(ox)_3][Cr(bpy)_3]ClO_4$ given in ref 2. Excitation at 568 or 532 nm with the Ar^+/Kr^+ ion laser or Nd:YAG laser, respectively, excites the $^4A_2 \rightarrow {}^4T_2$ transition of $[Cr(ox)_3]^{3-}$, while $[Cr(bpy)_3]^{3+}$ is essentially nonabsorbing at these wavelengths.[6] The $[Cr(ox)_3]^{3-}$ decays rapidly into the metastable ^2E state, which has an intrinsic lifetime of 1.3 ms and a luminescence quantum efficiency close to unity at low temperatures in the absence of energy transfer processes.[3] However, the $^2E \rightarrow {}^4A_2$ transition of $[Cr(ox)_3]^{3-}$ is resonant with the $^4A_2 \rightarrow {}^2T_1$ transition of $[Cr(bpy)_3]^{3+}$. Hence an excited $[Cr(ox)_3]^{3-}$ can either decay radiatively or transfer its energy to another $[Cr(ox)_3]^{3-}$ or to a $[Cr(bpy)_3]^{3+}$. Energy transfer from $[Cr(ox)_3]^{3-}$ to $[Cr(bpy)_3]^{3+}$ is irreversible at low temperatures, because $[Cr(bpy)_3]^{3+}$ rapidly undergoes internal conversion from the $^2T_1$ level to the ^2E level before decaying intrinsically to the $^4A_2$ ground state. The intrinsic decay of the $[Cr(bpy)_3]^{3+}$ luminescence occurs with a radiative lifetime of 5 ms and a luminescence quantum yield close to unity at low temperatures.

(a) Relative Steady-State Luminescence of $[Cr(ox)_3]^{3-}$ and $[Cr(bpy)_3]^{3+}$ at 1.5 K. Broad-band luminescence spectra of $[Cr(ox)_3]^{3-}$ and $[Cr(bpy)_3]^{3+}$ in the title compounds were

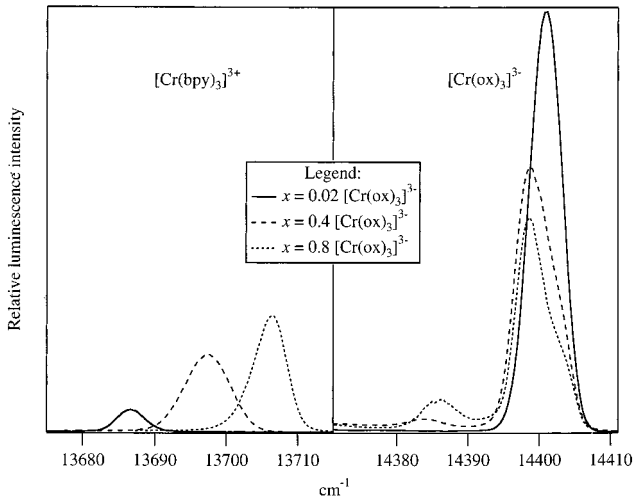

Figure 2. Representative relative steady-state luminescence spectra at 1.5 K for $[Cr(bpy)_3]^{3+}$ and $[Cr(ox)_3]^{3-}$ in $[NaAl_{1-x}Cr_x(ox)_3]$-$[Rh_{0.995}Cr_{0.005}(bpy)_3]ClO_4$, $x = 0.02$, 0.4, and 0.8, after $[Cr(ox)_3]^{3-}$ excitation at 568 nm.

obtained by CW irradiation at 568 nm and corrected for instrument response. Sample spectra for the $x = 0.02$, 0.4, and 0.8 $[Cr(ox)_3]^{3-}/y = 0.005$ $[Cr(bpy)_3]^{3+}$ systems at 1.5 K are shown in Figure 2 in the region of the respective R_1 lines. The zero-field splittings of the $^4A_2$ states are not resolved. The R_2 lines are not observed because the upper zero-field-split components of the respective ^2E states lie ~ 15 cm^{-1} higher in energy for both chromophores[2] and thus have negligible thermal populations at 1.5 K. Spectra were normalized to unity and the fraction of the total Cr^{3+} luminescence due to $[Cr(bpy)_3]^{3+}$ was plotted as a function of the effective $[Cr(ox)_3]^{3-}$ and $[Cr(bpy)_3]^{3+}$ concentrations for the two mixed-crystal series in Figures 3a and 4a, respectively.

In Figure 3a the relative intensity of the $[Cr(bpy)_3]^{3+}$ luminescence increases approximately linearly with $[Cr(ox)_3]^{3-}$ concentration for the $y = 0.005$ $[Cr(bpy)_3]^{3+}$ series. This increase is due to increasingly rapid resonant energy transfer from $[Cr(ox)_3]^{3-}$ to $[Cr(ox)_3]^{3-}$ and thus to more efficient feeding of $[Cr(bpy)_3]^{3+}$ traps as the $[Cr(ox)_3]^{3-}$ concentration increases. At low $[Cr(ox)_3]^{3-}$ concentration ($x \lesssim 0.02$) the $[Cr(bpy)_3]^{3+}$ contribution to the luminescence does not go to zero but levels off at $\sim$5%. Low $[Cr(ox)_3]^{3-}$ concentration means that the resonant energy transfer process assisting transfer to $[Cr(bpy)_3]^{3+}$ is negligible. The probability that a $[Cr(bpy)_3]^{3+}$ will occupy a site near to a $[Cr(ox)_3]^{3-}$ is constant for a given concentration of $[Cr(bpy)_3]^{3+}$, and hence a similar proportion of energy transfer from $[Cr(ox)_3]^{3-}$ to $[Cr(bpy)_3]^{3+}$ is expected for the $x \approx 0.001$ and $x \approx 0.02$ samples. In principle there could be a contribution to the $[Cr(bpy)_3]^{3+}$ luminescence due to direct excitation of weak vibrational sidebands of the spin−flip transitions of $[Cr(bpy)_3]^{3+}$. This contribution is negligible for excitation at 568 and 532 nm based on the following observations. (a) In absolute terms the luminescence intensity of $[Cr(bpy)_3]^{3+}$ falls off parallel to the $[Cr(ox)_3]^{3-}$ concentration down to $x \approx 0.02$. (b) Even at the lowest $[Cr(ox)_3]^{3-}$ concentration achievable of $x = 0.001$ the fraction of $[Cr(bpy)_3]^{3+}$ luminescence does not reincrease.

In Figure 4a, the linear dependence of the proportion of $[Cr(bpy)_3]^{3+}$ luminescence as a function of low $[Cr(bpy)_3]^{3+}$ concentration can be seen for the $x = 0.02$ $[Cr(ox)_3]^{3-}$ series. There is no measurable luminescence signal from $[Cr(bpy)_3]^{3+}$ in the nominally $y = 0$ sample, indicating that the effective $[Cr(bpy)_3]^{3+}$ concentration is very low indeed (Table 1).

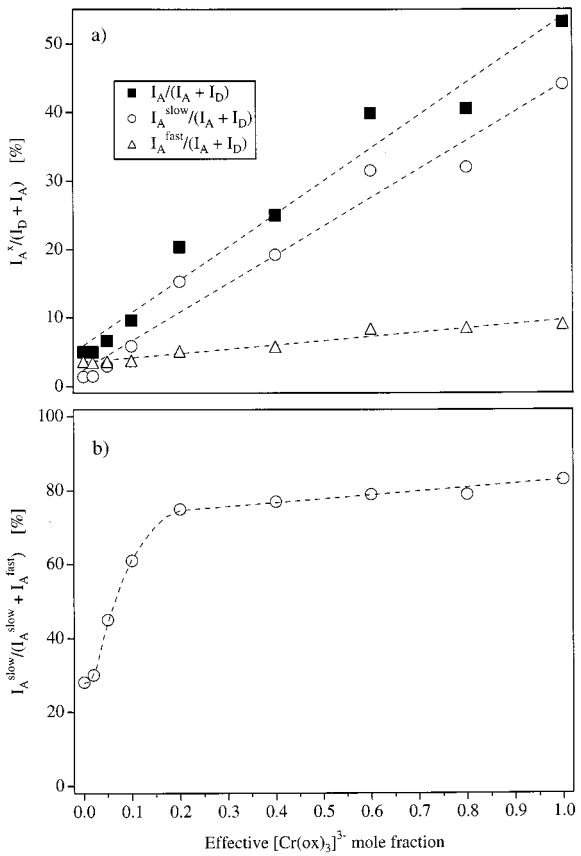

Figure 3. (a) The percentage of the total Cr^{3+} luminescence that arises from $[Cr(bpy)_3]^{3+}$ (■) as a function of $[Cr(ox)_3]^{3-}$ concentration for the $y = 0.005$ $[Cr(bpy)_3]^{3+}$ series, and the decomposition into the fast (Δ) and the slow (○) components, respectively. (b) The slow-rising fraction of the total $[Cr(bpy)_3]^{3+}$ luminescence taken from the curves in Figure 5. Dotted lines are a guide for the eye.

(b) Time-Resolved Luminescence of $[Cr(bpy)_3]^{3+}$ at 1.5 K. Time-resolved $[Cr(bpy)_3]^{3+}$ luminescence data for some samples in the $y = 0.005$ $[Cr(bpy)_3]^{3+}$ series are shown in Figure 5. The luminescence was monitored at the band maximum of the $[Cr(bpy)_3]^{3+}$ R_1 line, whose energy varies somewhat as a function of $[Cr(ox)_3]^{3-}$ concentration, from 13687 cm^{-1} for $x = 0.001$ to 13709 cm^{-1} for $x = 1$. There is a rise in the $[Cr(bpy)_3]^{3+}$ luminescence at short times followed by slow exponential decay with a lifetime of 5 ms. In Figure 5, $[Cr(ox)_3]^{3-}$ was excited at 568 nm by an $\sim$12-μs laser pulse. The rise has two distinct contributions: (i) a fast rise within the width of the laser pulse (labeled 1), which is *not* due to direct excitation (see above); and (ii) a slow rise on a millisecond time scale (labeled 2). Curves for the $x = 0.02$ $[Cr(ox)_3]^{3-}$ series are not shown here, because they are similar to the $x = 0.02$ $[Cr(ox)_3]^{3-}/y = 0.005$ $[Cr(bpy)_3]^{3+}$ sample.

Relative proportions of the fast- and slow-rising components were quantified by integration: The former was taken as a scaled curve with a sharp rise and an intrinsic decay of $\tau = 5$ ms, and the latter was the remainder shown as the gray curves in Figure 5. Figures 3b and 4b show the percentage of $[Cr(bpy)_3]^{3+}$ luminescence due to the slow-rising component as a function of the effective $[Cr(ox)_3]^{3-}$ and $[Cr(bpy)_3]^{3+}$ concentrations for the $y = 0.005$ $[Cr(bpy)_3]^{3+}$ and $x = 0.02$ $[Cr(ox)_3]^{3-}$ series, respectively. These data are also illustrated in Figures 3a and 4a as the fast and slow contributions to the *total* Cr^{3+} luminescence. For example, in the $x = 0.001$ and $x = 0.02$ $[Cr(ox)_3]^{3-}$ samples, $\sim$3.5% of the Cr^{3+} luminescence arises from $[Cr(bpy)_3]^{3+}$ that was excited by fast energy transfer from

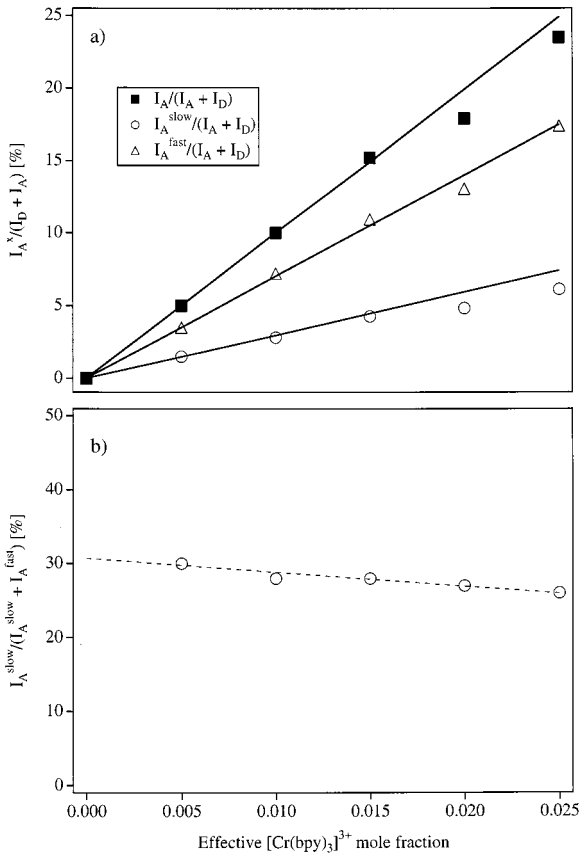

Figure 4. (a) The percentage of the total Cr^{3+} luminescence that arises from $[Cr(bpy)_3]^{3+}$ (■) as a function of $[Cr(bpy)_3]^{3+}$ concentration for the $x = 0.02$ $[Cr(ox)_3]^{3+}$ series, and its decomposition into the fast (Δ) and the slow (○) components, respectively. (—) Calculated on the basis of the combination of exchange-coupled, fast nearest-neighbor energy transfer and slow long-range transfer via a dipole−dipole mechanism. (b) The slow-rising fraction of the total $[Cr(bpy)_3]^{3+}$ luminescence. (− − −) Guide for the eye.

$[Cr(ox)_3]^{3-}$, and ∼1.5% is due to slow energy transfer, giving a total of 5% for the $[Cr(bpy)_3]^{3+}$ luminescence.

The contribution of the slow rise is almost identical for the $x = 0.001$ and $x = 0.02$ $[Cr(ox)_3]^{3-}$ samples in Figure 3b (∼30%), in agreement with the conclusion obtained from the relative luminescence data that the $[Cr(bpy)_3]^{3+}$ luminescence is not due to direct excitation. As concentration increases, the ratio shows two distinct regimes: (i) a rapid increase from ∼30% slow transfer for $x = 0.02$ $[Cr(ox)_3]^{3-}$ to ∼80% for $x \approx 0.3$, and (ii) only a very small further increase from $x = 0.3$ to $x = 1$. The $x = 0.02$ $[Cr(ox)_3]^{3-}$ samples, on the other hand, show a *slight* decrease in their slow transfer contribution over the small range of $[Cr(bpy)_3]^{3+}$ concentrations in Figure 4b.

The fast-rising component to the $[Cr(bpy)_3]^{3+}$ luminescence was partially resolved by using the 532-nm line of a pulsed Nd:YAG laser. Curves obtained for the $x = 0.05$ and $x = 1$ $[Cr(ox)_3]^{3-}/y = 0.005$ $[Cr(bpy)_3]^{3+}$ samples are shown in Figure 6. The one for $x = 0.05$ is typical for all values of $x \lesssim 0.1$. The resolved component, which we shall denote the "fast" rise and label "1 fast" in the figure, is single exponential at low $[Cr(ox)_3]^{3-}$ concentration, and yields an energy-transfer rate constant, $k_{et}^{fast} \approx 2 \times 10^6$ s^{-1}. With $x = 1$ the fast rise is no longer single exponential, because contributions from resonant $[Cr(ox)_3]^{3-}$ to $[Cr(ox)_3]^{3-}$ transfer[3] followed by rapid $[Cr(ox)_3]^{3-}$ to $[Cr(bpy)_3]^{3+}$ transfer become significant. The buildup of the nonresolved component, labeled "1 very fast"

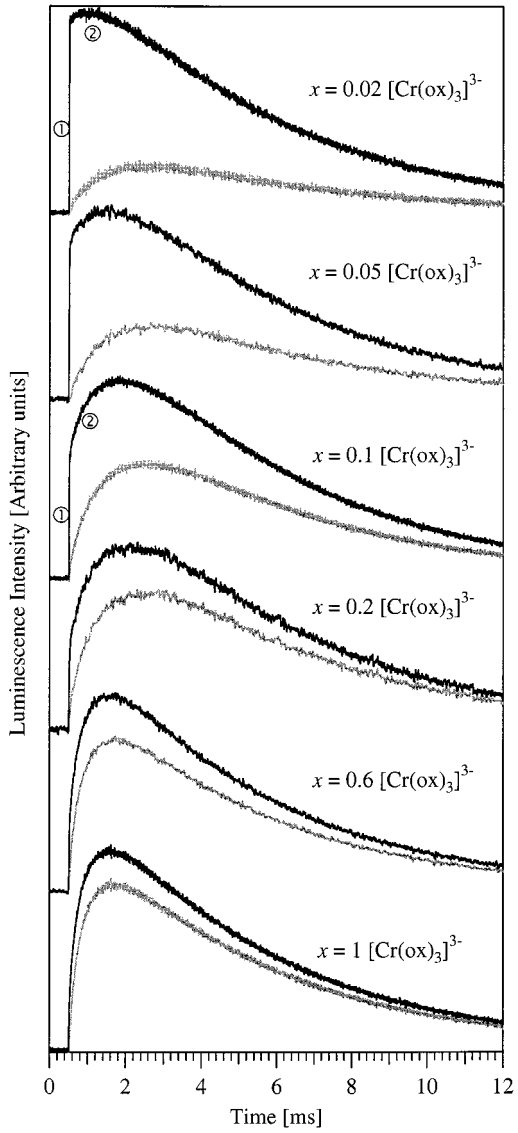

Figure 5. Time-resolved luminescence of $[Cr(bpy)_3]^{3+}$ excited at 568 nm for the $y = 0.005$ $[Cr(bpy)_3]^{3+}$ series. Black curves are the measured data, while gray curves show the slow-rising fraction proportion (labeled 2) after subtraction of the fast-rising component (1) and its decay.

in Figure 6, is complete within ∼50 ns, implying a $k_{et}^{v.fast} \geq 10^8$ s^{-1}. The resolved and nonresolved fast components have an intensity ratio of ∼3:4 for $[Cr(ox)_3]^{3-}$ concentrations $x \lesssim 0.1$.

Discussion

In the preceding section three distinct $[Cr(ox)_3]^{3-}$ to $[Cr(bpy)_3]^{3+}$ energy transfer processes occurring on very different time scales were identified. The outline of this section is as follows: First the two fast-rising components (1 in Figure 5) will be discussed and it is shown that a dipole−dipole mechanism for energy transfer from $[Cr(ox)_3]^{3-}$ to $[Cr(bpy)_3]^{3+}$ fails to fit the data. Instead superexchange coupling is proposed. In the second part, the slow rise (2 in Figure 5) at low $[Cr(ox)_3]^{3-}$ and $[Cr(bpy)_3]^{3+}$ concentrations is modeled by a dipole−dipole mechanism. Finally the energy-transfer behavior as a function of $[Cr(ox)_3]^{3-}$ and $[Cr(bpy)_3]^{3+}$ concentration is considered briefly.

The probability that energy transfer occurs from a donor D ($[Cr(ox)_3]^{3-}$) to an acceptor A ($[Cr(bpy)_3]^{3+}$) is given by the general equation:[7−9]

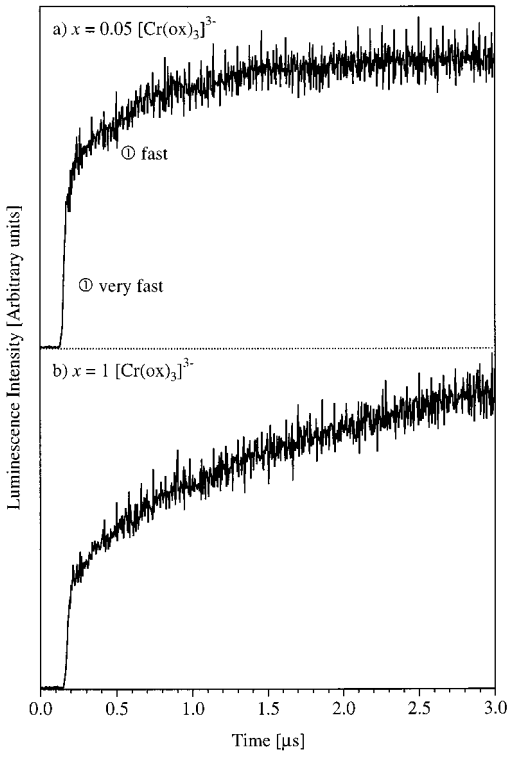

Figure 6. Partial resolution of the fast-rising component of the $[Cr(bpy)_3]^{3+}$ luminescence by using the Nd:YAG laser. Curves for $x = 0.05$ and $x = 1$ $[Cr(ox)_3]^{3-}$ ($y = 0.005$ $[Cr(bpy)_3]^{3+}$) are shown in panels (a) and (b), respectively. The resolved and nonresolved components are labeled "1 fast" and "1 very fast", respectively.

$$w_{DA} = \frac{2\pi}{\hbar}|\langle D, A^*|H'|D^*, A\rangle|^2\, \Omega_{DA} \tag{1}$$

H′ is the interaction Hamiltonian that mediates energy transfer from the excited donor D* to the unexcited acceptor. The interaction mechanism may be electrostatic, magnetic, and/or exchange coupling. Ω_{DA} is the spectral overlap of the transition in centimeters, and is necessary for energy conservation. It takes the form:

$$\Omega_{DA} = \int g_A(E)\, g_D(E)\, dE \tag{2}$$

where $g_A(E)$ and $g_D(E)$ are the normalized line shape functions for the homogeneous lines of the donor and acceptor, respectively. In the present case there is reasonable spectral overlap between the $^4A_2 \rightarrow {}^2E$ transition of $[Cr(ox)_3]^{3-}$ and the $^4A_2 \rightarrow {}^2T_1$ transition of $[Cr(bpy)_3]^{3+}$.

For an electric dipole−electric dipole mechanism eq 1 becomes[10]

$$w_{DA}^{d-d} = const \cdot \frac{Q_A \Omega_{DA}}{\tau_r^D R_{DA}^6 \tilde{\nu}_{DA}^4} = \frac{1}{\tau_{int}^D}\left(\frac{R_c}{R_{DA}}\right)^6 \tag{3}$$

with

$$R_c = \left(\frac{const\, Q_A \Omega_{DA} \eta_r^D}{\tilde{\nu}_{DA}^4}\right)^{1/6} \tag{4}$$

Q_A is the integrated absorption cross-section (in cm) of the acceptor transition, τ_r^D, τ_{int}^D (in s) and η_r^D are the radiative lifetime, the intrinsic lifetime, and the luminescence quantum efficiency of the donor in the absence of energy transfer, respectively, R_{DA} is the donor−acceptor separation (in cm), and $\tilde{\nu}_{DA}$ is the resonance frequency (in cm^{-1}). *const* collects fundamental constants and takes on a value of 2.7×10^{-5} with the other quantities in the above units. R_c is the critical donor−acceptor separation for which the probability of energy transfer is equal to the probability of intrinsic decay of the donor.

The actual rate constant of energy transfer for a given donor depends on the distribution of accessible acceptors according to

$$k_{et} = \sum_A w_{DA} \tag{5}$$

In a mixed-crystal system, k_{et} differs from donor to donor according to each donor's specific acceptor environment. The total quantum efficiency for energy transfer from the ensemble of donors is given by:

$$\eta_{et}^{tot} = \frac{1}{N_D}\sum_D \eta_{et}^D = \frac{1}{N_D}\sum_D \frac{k_{et}^D}{k_{int}^D + k_{et}^D} \tag{6}$$

where the sum goes over all donors D and N_D is the total number of donors. In the case of quantum efficiencies for intrinsic luminescence of both donor and acceptor close to unity,

$$\eta_{et}^{tot} = \frac{I_A}{I_A + I_D} = \frac{I_A}{I_{tot}} \tag{7}$$

where I_A and I_D are the luminescence intensities of the acceptor and the donor expressed in photons/s, respectively.

For the diluted system with $x = 0.02$ $[Cr(ox)_3]^{3-}$ and $y = 0.005$ $[Cr(bpy)_3]^{3+}$, $\eta_{et}^{tot} = 5\%$ can unambiguously be separated into a fast contribution $\eta_{et}^{fast} = 3.5\%$ and a slow contribution $\eta_{et}^{slow} = 1.5\%$.

(a) Fast Rise. Irrespective of the nature of the interaction between donors and acceptors, the fast rise to the $[Cr(bpy)_3]^{3+}$ luminescence in the system containing effectively $x = 0.02$ of $[Cr(ox)_3]^{3-}$ donors and $y = 0.005$ of $[Cr(bpy)_3]^{3+}$ acceptors must be due to transfer from excited $[Cr(ox)_3]^{3-}$ complexes which happen to have a $[Cr(bpy)_3]^{3+}$ complex within the nearest-neighbor shell of acceptor sites with R_{DA} between 6.1 and 9.1 Å. Now it can be easily demonstrated that this fast rise cannot be attributed to electrostatic coupling of ions via an electric dipole−electric dipole interaction. If such were the case, then R_c would take on a hypothetical value > 40 Å, using $k_{et} > 10^8$ s^{-1} from the very fast component of the fast rise in Figure 6, the shortest distance between donor and acceptor within the first shell $R_{DA} = 6.1$ Å, and $\tau_{int}^D = \tau_r^D = 1.3$ ms. With such a large value of R_c, the total intensity of the $[Cr(bpy)_3]^{3+}$ luminescence would, however, have to amount to more than 99% of the total luminescence because even for the low acceptor concentration of $y = 0.005$, every donor would have more than one acceptor within a radius of 40 Å. This is in contrast to the observed fraction of only 5% shown in Figure 3a. Hence the fast rise cannot be due to a dipole−dipole mechanism.

As an alternative, superexchange coupling between $[Cr(ox)_3]^{3-}$ and nearby $[Cr(bpy)_3]^{3+}$ is considered as a possible explanation for the observed fast rise to the $[Cr(bpy)_3]^{3+}$ luminescence. In this case the interaction Hamiltonian H′ in eq 1 has the form[11,12]

$$H'_{ex} = -2\sum_{i,j} J_{ij}\, \boldsymbol{s}_i^a \cdot \boldsymbol{s}_j^b \tag{8}$$

J_{ij} is the exchange integral corresponding to an interaction between two electrons on centers a and b, and s_i^a and s_j^b are spin angular momentum operators for the electrons.

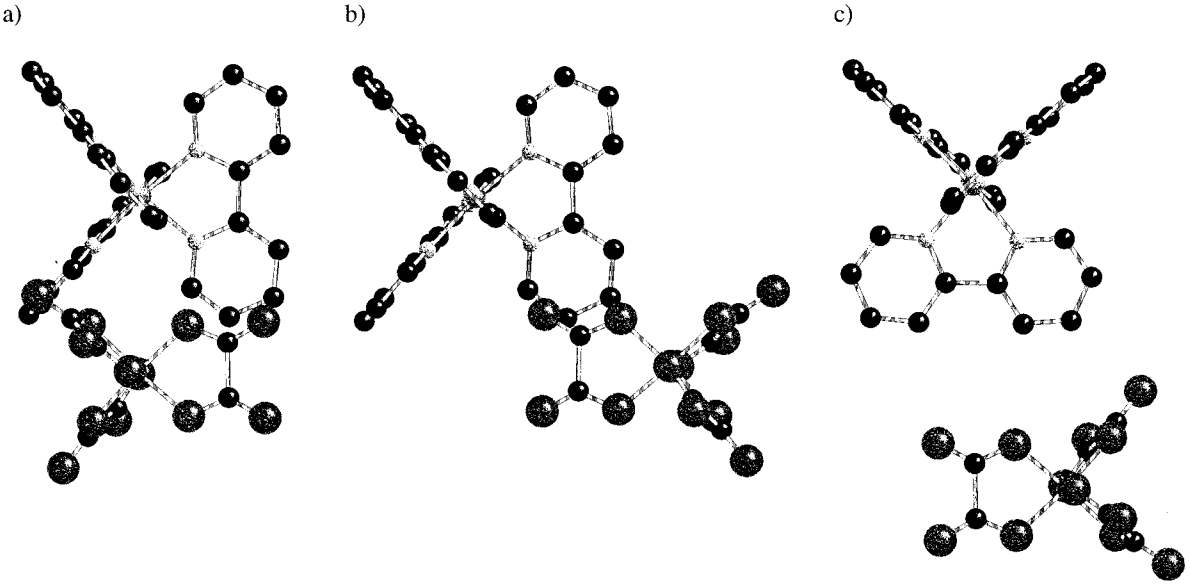

Figure 7. Views of $[Cr(ox)_3]^{3-}$ and $[Cr(bpy)_3]^{3+}$ from above the ligand plane for (a) the 6.1 Å, (b) the 8.5 Å, and (c) the 9.1 Å pairs, taken from the published structure.[2] For further details, see the text.

Superexchange coupling falls off much more rapidly with R_{DA} than the dipole−dipole interaction. In addition, it requires a specific pathway to mediate it. For the compounds under discussion, it is proposed that $\pi-\pi$ interactions between the oxalate and bpy ligands provide a pathway for superexchange coupling between the Cr^{3+} ions of $[Cr(ox)_3]^{3-}$ and $[Cr(bpy)_3]^{3+}$ within the above-mentioned nearest-neighbor shell. For larger values of R_{DA} there is no such pathway and superexchange coupling can safely be neglected. Since an estimate for the actual coupling matrix element in eq 1 using H'_{ex} from eq 8 is difficult for such a superexchange mechanism, some previous literature estimates for the magnitude of exchange couplings and the corresponding energy-transfer rate constants are briefly considered in the following. Riesen and Güdel investigated energy transfer between Cr^{3+} dimers in $[(NH_3)_5CrOHCr(NH_3)_5]Cl_5 \cdot H_2O$.[13] In their system all bonding is σ-type within dimers. Between dimers there are ionic and hydrogen bonds, and the shortest interdimer distance is 7.27 Å. Nevertheless, they estimated that an interaction energy of ~ 0.02 cm^{-1} between dimers would give rise to their observed energy transfer rate constant $k_{et} \approx 10^6$ s^{-1} at 100 K. Earlier Huang[12] considered collinear pairs of $(3d^3)$ V^{2+} ions in $KMgF_3$, where each V^{2+} is separated by one to three F^- ions. Superexchange energy transfer integrals over one intervening F^- ion were estimated to be ~ 7 cm^{-1}. Interaction energies were estimated to decrease by a factor of $\sim 10^2$ for superexchange via each additional F^- ion, yielding a small exchange interaction of $\sim 10^{-3}$ cm^{-1} when two V^{2+} ions are separated by three F^- ions. Even such a small coupling was considered large enough to result in $k_{et} \approx 10^6$ s^{-1}.

Hence, although superexchange interactions occur only over a short distance in the crystal, and are quite weak in the absence of direct bridging ligands ($\sim 10^{-3} - 10^{-2}$ cm^{-1}), they may lead to rapid energy transfer. Applying these results to the present system suggests that a superexchange interaction energy of $10^{-3}-10^{-2}$ cm^{-1} is responsible for the resolved fast energy transfer process, $k_{et}^{fast} \approx 2 \times 10^6$ s^{-1}. For the nonresolved, very fast component with $k_{et}^{v.fast} \geq 10^8$ s^{-1}, an upper limit of ~ 0.2 cm^{-1} can in fact be estimated by comparison with FLN data, where Heisenberg-type exchange was incorporated in the analysis of the ground-state zero-field splitting.[4]

Although rapid, the short effective range of superexchange interactions means that energy transfer from $[Cr(ox)_3]^{3-}$ to $[Cr(bpy)_3]^{3+}$ occurs only for $[Cr(ox)_3]^{3-}$ that have a $[Cr(bpy)_3]^{3+}$ acceptor in the nearest-neighbor shell. Seven acceptor sites lie within 9.1 Å of a given $[Cr(ox)_3]^{3-}$. For the $x = 0.02$ $[Cr(ox)_3]^{3-}/y = 0.005$ $[Cr(bpy)_3]^{3+}$ sample there is a 3.5% probability that one of these sites is populated by a $[Cr(bpy)_3]^{3+}$ complex, and thus for $k_{et} \gg k_{int}^D = 1/\tau_r^D$ and $\eta_r^D = \eta_r^A \approx 1$, the superexchange model predicts that $\eta_{et}^{fast} = 3.5\%$, and that therefore 3.5% of the total luminescence should arise from fast energy transfer to $[Cr(bpy)_3]^{3+}$. This is in agreement with the measured value of $I_A^{fast}/I_{tot} = 3.5\%$ shown in Figure 3a. Furthermore, at low $[Cr(bpy)_3]^{3+}$ acceptor concentration the superexchange model predicts a linear dependence of η_{et}^{fast} on the acceptor concentration with a slope of $7y$, in accordance with experimental observations (see Figure 4a). This result provides direct evidence that superexchange energy transfer only occurs to the first shell of seven acceptor sites. In further agreement with this mechanism is the work of Decurtins et al.,[2] who found that for the neat $[Cr(bpy)_3]^{3+}$ system ($x = 1$) the relative luminescence of $[Cr(ox)_3]^{3-}$ and $[Cr(bpy)_3]^{3+}$ favors the latter by a ratio of $\sim 6 \times 10^{-5}$:1. In this case, every $[Cr(ox)_3]^{3-}$ has a nearby $[Cr(bpy)_3]^{3+}$, and thus energy transfer to $[Cr(bpy)_3]^{3+}$ is rapid and almost complete.

The crystal structure also lends qualitative support to a superexchange mechanism with two components: one very fast and nonresolvable, while the other is somewhat slower and resolvable. The structure of the 3D oxalate networks with space group $P2_13$ and the incorporated $[M^{III}(bpy)_3]^{3+}$ is well-known.[2] The seven $[M^{III}(bpy)_3]^{3+}$ sites within the first neighbor shell fall into three subshells. There is one site at 6.1 Å, three at 8.5 Å, and three at 9.1 Å. Each of these subshells is now considered in turn.

In the nearest-neighbor pair the two complexes sit on top of one another on the same trigonal axis. Figure 7a shows one of three equivalent interactions between oxalate and bipyridine ligands. The ligands lie in canted planes (approximately 10° off parallel) ~ 3.45 Å apart, with a closest atom approach of 3.67 Å. Reasonable π overlap seems likely, providing a good superexchange pathway. A similar conclusion is drawn for the 8.5 Å pairs, one of which is pictured in Figure 7b. Although the Cr^{3+} are on the opposite side (cf. Figure 7a) and only one pair of ligands interact, the separation (~ 3.45 Å) and canting of the planes ($\sim 7°$) are similar to the 6.1 Å case, as is the closest

TABLE 2: Parameters and Corresponding Dipole−Dipole Energy Transfer Rate Constants k_{et}^D for the Slow Rise to the $[Cr(bpy)_3]^{3+}$ Luminescence Calculated by Using Eq 6 with $R_c = 10.6$ Å for the Three Next-Nearest Shells of Acceptor Sites

shell	range of R_{DA} in group (Å)	number of sites	average R_{DA} (Å)	k_{et}^D (s^{-1})
1	6.1−9.1	7	8.4	N/A
2	12.84−13.8	9	13.3	197
3	17.15−18.1	15	17.5	38
4	19.6−20.95	22	20.5	15

atom approach of 3.66 Å. An example of one of the 9.1 Å pairs is given in Figure 7c. Here the bpy ligand makes quite a close approach to, and lies in the same plane as the Cr^{3+} of $[Cr(ox)_3]^{3-}$. However, π overlap is much reduced, providing a poorer superexchange pathway.

On the basis of these observations, it is reasonable to conclude that the rate of energy transfer between $[Cr(ox)_3]^{3-}$ and $[Cr(bpy)_3]^{3+}$ pairs separated by 6.1 and 8.4 Å is so fast as to be unresolved in the present experiments, whereas it is slower and resolvable ($\sim 2 \times 10^6$ s^{-1}) for the 9.1 Å pairs. This analysis would predict a ratio of 3:4 for the resolved:nonresolved fast transfer processes, as is observed experimentally.

(b) Slow Rise for the Sample Series with Low Oxalate Concentration. In this subsection it is shown that the slow-rising component of the $[Cr(bpy)_3]^{3+}$ luminescence at low $[Cr(ox)_3]^{3-}$ concentration is consistent with an electric dipole − electric dipole mechanism for the energy transfer from $[Cr(ox)_3]^{3-}$ to $[Cr(bpy)_3]^{3+}$.

As mentioned above the intrinsic quantum yields of both the $[Cr(ox)_3]^{3-}$ donor as well as the $[Cr(bpy)_3]^{3+}$ acceptor, η_r^D and η_r^A, are close to unity at 1.5 K. Thus, for the former the intrinsic decay rate constant $k_{int}^D = 1/\tau_r^D = 770$ s^{-1}, while for the latter $k_{int}^A = 1/\tau_r^A = 200$ s^{-1}. For the $x = 0.02$ $[Cr(ox)_3]^{3-}$ and $y = 0.005$ $[Cr(bpy)_3]^{3+}$ sample, the experimental quantum efficiency of the slow donor to acceptor energy transfer $\eta_{et}^{slow} = I_A^{slow}/I_{tot} = 1.5\%$.

Theoretically η_{et}^{slow} is given by eq 6, where the sum is taken over all donors with the exception of those having an acceptor in the nearest-neighbor shell accounted for in the preceding section. Apart from the first seven $[M^{III}(bpy)_3]^{3+}$ sites assigned to the first shell, the further $[M^{III}(bpy)_3]^{3+}$ sites can be grouped into shells corresponding to second, third, fourth, and so-forth nearest neighbors,[14] each shell containing a number n_i of sites in a small range around an average value of R_{DA}^i. In Table 2 values for R_{DA}^i and n_i are given for up to the fourth nearest-neighbor shells. For the very low acceptor concentration of $y = 0.005$, the probability for the occupancy of a given shell by just one acceptor is simply $p_i \approx n_i y$, and double occupancy is negligible. If R_c is not too large, the sum in eq 6 has only nonzero contributions for the first few shells. In this case the quantum efficiency for the slow energy transfer with $k_{et}^D = w_{DA}^{d-d}$ according to eq 3 takes on the form

$$\eta_{et}^{slow} = y \sum_{i=2}^{4} n_i \frac{(R_{DA}^i/R_c)^6}{1 + (R_{DA}^i/R_c)^6} \qquad (9)$$

With η_{et}^{slow} given by the experimental value of 1.5%, this equation can be solved implicitly, resulting in a value of $R_c = 10.6$ Å, which in retrospect justifies the neglect of acceptors at values for $R_{DA} > 21$ Å.

This value for R_c has to be compared to the one predicted on the basis of eq 5. Unfortunately there are rather large uncertainties in determining the integrated absorption cross-section Q_A and the spectral overlap integral Ω_{DA}. Nevertheless, order-of-magnitude estimates should be possible. The relevant spectral overlap is between the electronic origin of the $^4A_2 \rightarrow {}^2E(R_1)$ donor transition and a vibrational sideband of the $^4A_2 \rightarrow {}^2T_1$ acceptor transition. Whereas for the former the homogeneous line width $\Gamma_{hom} = 0.012$ cm^{-1} is known,[3] the pertinent parameters for the latter can only be roughly estimated. Vibrational sidebands of the $^4A_2 \rightarrow {}^2T_1$ transition are weak, typically with extinction coefficients $\epsilon \lesssim 0.5$ l mol^{-1} cm^{-1} and halfwidths $\Delta\tilde{\nu}_{1/2}$ on the order of 10 cm^{-1} (see spectra in ref 6), resulting in values of $Q_A \approx 10^{-20}$ cm (oscillator strength $f \approx 10^{-8}$) and $\Omega_{DA} \approx 0.1$ cm. Together with the resonance frequency $\tilde{\nu}_{DA} = 14400$ cm^{-1}, eq 4 gives $R_c \approx 10$ Å, which is in agreement with the experimental value.

In the simple model, η_{et}^{slow} depends linearly upon the acceptor concentration y with the slope determined by R_c. The corresponding curve calculated with $R_c = 10.6$ Å is shown in Figure 4a for the series $x = 0.02/y = 0.005$ to $y = 0.025$. The data are very well explained at low concentrations, but as the concentration increases there is a small deviation of the experimental points from the linear behavior because multiple occupancies begin to play a role. As there are fewer acceptor sites for the fast transfer process, η_{et}^{fast} is less susceptible to multiple occupancies at low concentrations than is η_{et}^{slow}, and the relative contribution of η_{et}^{slow} to η_{et}^{fast} decreases slightly with $[Cr(bpy)_3]^{3+}$ concentration as is evident in Figure 4b.

Table 2 includes k_{et}^D obtained with $R_c = 10.6$ Å for the second to fourth nearest-neighbor shells. With these rate constants the time-resolved luminescence of the $[Cr(bpy)_3]^{3+}$ acceptor for the $x = 0.02/y = 0.005$ sample can be easily computed. In the absence of $[Cr(ox)_3]^{3-}$-to-$[Cr(ox)_3]^{3-}$ energy migration, with negligible direct excitation of $[Cr(bpy)_3]^{3+}$ and neglecting double occupancies of acceptor sites within the four shells around a given donor, the time-dependence of the excited-state population of $[Cr(bpy)_3]^{3+}$ for each shell, N_e^A, can be described by the rate equation[7]

$$\frac{dN_e^A}{dt} = -k_{int}^A N_e^A + N_e^D(t=0) \cdot k_{et}^D \cdot \exp[-(k_{int}^D + k_{et}^D)t] \qquad (10)$$

$N_e^D(t=0)$ is the number of excited donors at $t = 0$, and $k_{int}^A = 200$ s^{-1} is the intrinsic decay rate constant of $[Cr(bpy)_3]^{3+}$. Solving eq 10 yields

$$N_e^A = \frac{N_e^D(t=0) \cdot k_{et}^D}{(k_{int}^D + k_{et}^D) - k_{int}^A} \cdot \{\exp[-k_{int}^A \cdot t] - \exp[-(k_{int}^D + k_{et}^D)t]\} \qquad (11)$$

The total excited-state population of acceptors for the slow energy transfer as a function of time is just a weighted sum over second-to fourth-neighbor shells of eq 11. In Figure 8 the experimental slow rise and the curve calculated as described above are displayed. The agreement between the two is excellent. Because all values for k_{et}^D in Table 2 are smaller than the intrinsic decay rate constant of the donor, the rise time is very close to the limiting value of $k_{int}^D = 770$ s^{-1}.

On the basis of the good agreement between the experimental and theoretical results, the slow rise to the $[Cr(bpy)_3]^{3+}$ luminescence is attributed to a dipole−dipole mechanism involving acceptors at distances between 12.5 and 21 Å, having no reasonable pathway for superexchange.

(c) Ratio of Slow to Fast Transfer as a Function of $[Cr(ox)_3]^{3-}$ Concentration. Finally, an explanation is sought

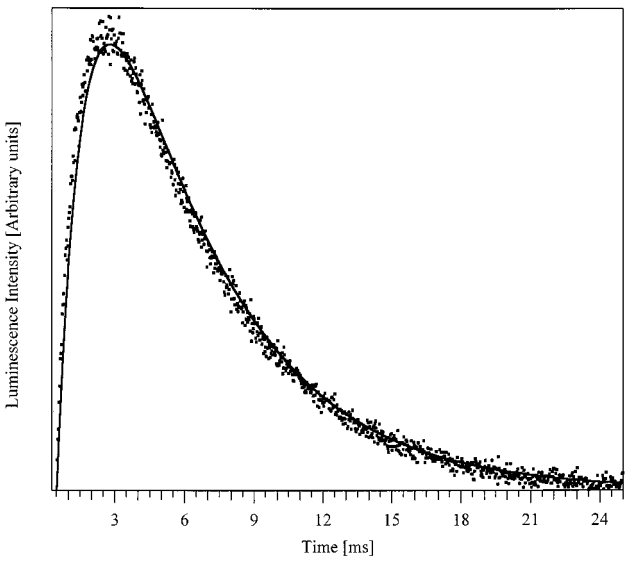

Figure 8. Experimental points for the slow-rising component to the time-resolved luminescence of $[NaAl_{0.98}Cr_{0.02}(ox)_3][Rh_{0.995}Cr_{0.005}(bpy)_3]ClO_4$ and the curve calculated using a simplified shell model.

as to why both the total luminescence of $[Cr(bpy)_3]^{3+}$ and the proportion of the luminescence due to slow energy transfer increase with $[Cr(ox)_3]^{3-}$ concentration (see Figure 3b). These effects are almost certainly due to resonant multistep transfer[3] from isolated $[Cr(ox)_3]^{3-}$ centers to a $[Cr(ox)_3]^{3-}$ with a nearby $[Cr(bpy)_3]^{3+}$, followed by rapid energy transfer to this $[Cr(bpy)_3]^{3+}$ acting as a deep trap. Hence the importance of dipole−dipole energy transfer from $[Cr(ox)_3]^{3-}$ to $[Cr(bpy)_3]^{3+}$ decreases with increasing $[Cr(ox)_3]^{3-}$ concentration.

Assuming constant $[Cr(bpy)_3]^{3+}$ concentration, one would expect that the fast-rising contribution remains constant irrespective of the $[Cr(ox)_3]^{3-}$ concentration. As plotted in Figure 3a, this is not entirely the case, but a slight rise with $[Cr(ox)_3]^{3-}$ concentration is observed. This could of course be due to an unwanted increase in the fraction of $[Cr(bpy)_3]^{3+}$ incorporated into the mixed crystals with increasing $[Cr(ox)_3]^{3-}$ concentration. In view of the relative stabilities of the two complexes this seems unlikely. Rather, at higher oxalate concentrations there is a contamination of the fast-rising component by some other process, as for instance just one fast resonant energy transfer step from one $[Cr(ox)_3]^{3-}$ to another, followed by the rapid energy transfer to $[Cr(bpy)_3]^{3+}$. This is evident in Figure 6 from the differing shapes of the fast rises of the $x = 0.05$ and $x = 1$ $[Cr(ox)_3]^{3-}$ samples. On the time scale of the data in Figure 5, from which the partitioning was obtained, this contribution would be significant, thus overestimating the fraction due to the single-step fast rise. It is concluded that the energy-transfer contribution due solely to superexchange is constant, and that a linear increase in the proportion of $[Cr(bpy)_3]^{3+}$ luminescence is observed due to resonant energy transfer in the $[Cr(ox)_3]^{3-}$ network mediating transfer to $[Cr(bpy)_3]^{3+}$.

Conclusion

Energy transfer from $[Cr(ox)_3]^{3-}$ in 3D oxalate networks to encapsulated $[Cr(bpy)_3]^{3+}$ was observed in steady-state and time-resolved luminescence experiments. Two mechanisms for transfer were identified from the time-resolved data. Rapid, short-range transfer ($k_{et}^{exch} > 10^6$ s^{-1}) was attributed to superexchange coupling between Cr^{3+} ions in the first shell via π overlap of the oxalate and bipyridine ligands. Pairs of ligands in the two nearest-neighbor subshells of this shell, with four available sites in total, have significantly more overlap than the third subshell with three sites, and are responsible, respectively, for the nonresolved ($\geq 10^8$ s^{-1}) and resolved components ($\sim 2 \times 10^6$ s^{-1}) to the fast rise. The short effective range of the superexchange mechanism accounts for the low level of steady-state luminescence obtained at low $[Cr(bpy)_3]^{3+}$ concentration.

A very much slower process was easily separated from the fast process at low oxalate concentration ($x = 0.02$). It has been attributed to a dipole−dipole mechanism by comparison with the results of a simplified shell model,[14] using a value for $R_c = 10.6$ Å.

At higher $[Cr(ox)_3]^{3-}$ concentrations, resonant $[Cr(ox)_3]^{3-}$-to-$[Cr(ox)_3]^{3-}$ energy transfer[3] also assists $[Cr(ox)_3]^{3-}$-to-$[Cr(bpy)_3]^{3+}$ transfer by moving the excitation energy from isolated $[Cr(ox)_3]^{3-}$ to those with a nearby $[Cr(bpy)_3]^{3+}$, thus increasing the fraction of luminescence due to $[Cr(bpy)_3]^{3+}$.

In other well-investigated Cr^{3+}-containing systems, as for instance ruby ($Al_2O_3:Cr^{3+}$), the distinction between different mechanisms is less evident.[15−17] In such doped oxides the situation is more complicated because of the various superexchange pathways across the bridging oxygen atoms. In lightly doped ruby this leads to the formation of exchange-coupled pairs and so-called N line luminescence at lower energy than the single-ion R lines. The single ions act as donors, the pairs act as acceptors in much the same way as $[Cr(ox)_3]^{3-}$ and $[Cr(bpy)_3]^{3+}$ in our system. This energy transfer was proposed to proceed via an superexchange mechanism across the bridging oxygen atoms also for larger distances than for the four nearest-neighbor distances identified in the N lines.[15] But it cannot be excluded that multi-pole interaction does not play a nonnegligible role. In addition, single-ion energy transfer is dominated by phonon-assisted processes.[15] In heavily doped ruby ($Cr^{3+} > 1\%$), there is the added complication of the formation of polynuclear Cr^{3+} clusters, leading to luminescence at still lower energies than the N lines.[17] The number of different species and the number of processes to be taken into consideration in a quantitative evaluation of the experimental data are thus quite large. Ruby therefore constitutes a much more complicated system than appears at first glance, particularly since the relative concentrations of the different species cannot be varied independently of each other.

In the system presented here, the evidence for two competing mechanisms for energy transfer from $[Cr(ox)_3]^{3-}$ to $[Cr(bpy)_3]^{3+}$ is clear-cut. This is basically due to the fact that the two mechanisms have very different dependencies on the donor−acceptor separation in conjunction with the specific shell structure of our compound, with an extremely noncontinuous distribution in the donor−acceptor separation. This leads to the many orders of magnitude difference in rate constants of the two mechanisms, and allows them to be separated experimentally. The fact that acceptors and donors can be incorporated into the host lattice at concentrations which are independent of each other allows a quantitatively coherent evaluation of the experimental data. In other systems with a more continuous distribution of donor−acceptor separations, an experimental differentiation of the two mechanisms might prove inherently more difficult.

Acknowledgment. We thank N. Amstutz of the Université de Genève for preparation of the samples, B. Frei of the Universität Bern for the determination of sample concentrations, and S. Decurtins and R. Pellaux of Universität Bern for their advice. Gratitude is also expressed to the Swiss National Science

Foundation and the "Fondation Ernst et Lucie Schmidheiny" for financial support.

References and Notes

(1) Decurtins, S.; Schmalle, H. W.; Schneuwly, P.; Ensling, J.; Gütlich, P. *J. Am. Chem. Soc.* **1994**, *116*, 9521.

(2) Decurtins, S.; Schmalle, H. W.; Pellaux, R.; Schneuwly, P.; Hauser, A. *Inorg. Chem.* **1996**, *35*, 1451.

(3) von Arx, M. E.; Hauser, A.; Riesen, H.; Pellaux, R.; Decurtins, S. *Phys. Rev. B* **1996**, *54*, 15800.

(4) Langford, V. S.; Hauser, A.; Riesen, H. Manuscript in preparation.

(5) Oetliker, U. MEASURE Software for Laboratory Instrument Control and Data Acquisiton; Geneva, 1998, for additional information contact Ulrich. Oetliker@chiphy.unige.ch.

(6) Hauser, A.; Mäder, M.; Robinson, W. T.; Murugesan, R.; Ferguson, J. *Inorg. Chem.* **1987**, *26*, 1331.

(7) Henderson, B.; Imbusch, G. F. *Optical Spectroscopy of Inorganic Solids*; Oxford University Press: Oxford, 1989.

(8) Smets, B. In *Optical Properties of Excited States in Solids*, NATO ASI B301; di Bartolo, B. ed.; Plenum Press: New York, 1992.

(9) Blasse, G.; Grabmaier, B. C. *Luminescent Materials*; Springer-Verlag: Berlin, 1994.

(10) Blasse, G. *Phillips Res. Rep.* **1969**, *24*, 131.

(11) Birgeneau, R. J. *J. Chem. Phys.* **1969**, *50*, 4282.

(12) Huang, N. L. *Phys. Rev. B* **1970**, *1*, 945.

(13) Riesen, H.; Güdel, H. U. *Mol. Phys.* **1986**, *58*, 509.

(14) Vasquez, S. O.; Flint, C. D. *Chem. Phys. Lett.* **1995**, *238*, 378.

(15) Selzer, P. M.; Huber, D. L.; Barnett, B. B.; Yen, W. M. *Phys. Rev. B* **1978**, *17*, 4979.

(16) Imbush, G. F.; Yen, W. M. In *Laser spectroscopy and new ideas*; Yen, W. M., Levenson, M. D., Eds; Springer Series in Optical Sciences 54, Berlin 1987, p 248.

(17) Jamison, S. P.; Imbush, G. F. *J. Lumin.* **1997**, *75*, 143.